Metals **2014**, *4*, 401-409; doi:10.3390/met4030401

OPEN ACCESS

metals

ISSN 2075-4701

www.mdpi.com/journal/metals/

Article

Fabrication and Mechanical Characterisation of Titanium Lattices with Graded Porosity

William van Grunsven [1], Everth Hernandez-Nava [2], Gwendolen C. Reilly [1,3] and Russell Goodall [2,*]

[1] Department of Materials Science and Engineering, Kroto Research Institute, University of Sheffield, Broad Lane, Sheffield S3 7HQ, UK; E-Mails: w.vangrunsven@gmail.com (W.G.); g.reilly@sheffield.ac.uk (G.C.R.)

[2] Department of Materials Science and Engineering, University of Sheffield, Sir Robert Hadfield Building, Mappin St, Sheffield S1 3JD, UK; E-Mail: mtq10eh@sheffield.ac.uk

[3] Insigneo Institute for *in silico* Medicine, University of Sheffield, Pam Liversidge Building, Mappin St, Sheffield S1 3JD, UK

* Author to whom correspondence should be addressed; E-Mail: r.goodall@sheffield.ac.uk; Tel.: +44-0-114-222-5977; Fax: +44-0-114-222-5943.

Received: 3 July 2014; in revised form: 22 July 2014 / Accepted: 8 August 2014 / Published: 14 August 2014

Abstract: Electron Beam Melting (EBM) is an Additive Manufacturing technique which can be used to fabricate complex structures from alloys such as Ti6Al4V, for example for orthopaedic applications. Here we describe the use of EBM for the fabrication of a novel Ti6Al4V structure of a regular diamond lattice incorporating graded porosity, achieved via changes in the strut cross section thickness. Scanning Electron Microscopy and micro computed tomography analysis confirmed that generally EBM reproduced the CAD design of the lattice well, although at smaller strut sizes the fabricated lattice produced thicker struts than the model. Mechanical characterisation of the lattice in uniaxial compression showed that its behaviour under compression along the direction of gradation can be predicted to good accuracy with a simple rule of mixtures approach, knowing the properties and the behaviour of its constituent layers.

Keywords: Ti6Al4V; metal lattices; graded structure; mechanical properties; implant

---

1. Introduction

Porous metals in various forms, including foams and lattices, have been investigated for many years for a wide range of applications [1–3]. These range from lightweight structures to functional applications such as heat exchangers or electrodes.

For more than 25 years, porous metals in various forms have also successfully been applied in orthopaedics, where both structural (load support) and functional (biocompatible) properties are crucial to long term success. There has been significant progress in understanding the structure-property relationships of porous metals with a stochastic structure [4–6] and regular lattices [7], and how changes to this structure, beyond what can normally be controlled during processing, affect the behaviour (e.g., by the addition of a coating [8,9]). This has become more complex because of the wide variety of processing methods used to create these materials which give many subtle, but important, differences between structures. Until recently, the processing methods used allowed limited investigation of more complex controlled structures, but with advances in processing technology this is improving.

Electron Beam Melting (EBM) is a type of additive manufacturing which has recently attracted much attention for its potential to produce highly regular metallic lattices [10,11]. Over the last few years several types of uniform lattices have been built using EBM and similar techniques. Heinl *et al.* and Murr *et al*. suggested the use of porous metal lattices for orthopaedic applications and more recently several groups showed *in vitro* cell culture and *in vivo* implantation data for different lattices [12–15]. However, the great versatility of the process leaves many potential designs unexplored.

In this study, we describe the fabrication and the structural and mechanical analysis of a lattice with a graded architecture produced by EBM. We envisage that, among other applications, such a lattice could have a role in orthopaedic implants, where the higher stiffness core will be load bearing, while the more porous outer layers reduce the overall implant stiffness and would allow extensive bone ingrowth. A smooth gradation in structure between the core and periphery avoids a sharp interface where high stresses can have a negative effect on tissue ingrowth and mineralisation. This could lead to the formation of a more stable bone-implant interface with a reduced risk of failure. To date, some investigations on the mechanical [16,17] and thermal [18] properties of stochastic metal foams with structures graded in density or pore size have been reported, but the possibilities for lattices remain unexplored.

2. Experimental Methods

2.1. Fabrication

Four different lattices were designed in CAD to compare the mechanical properties of graded and uniform lattices. For orthopedic applications, the desirable pore size is small (the limit is approximately 300 microns [19]), so lattices were constructed with unit cells of 2 mm side length, close to the smallest dimensions that could be processed with good shape definition in the machine. Due to the need for unmelted powder to be removed, it was found in practice that relatively few layers could be made before the structure could not be fully cleaned. The sizes produced were representative

of possible use in implants as a graded transition layer, but it is important to note that the specimens created do not satisfy the normal requirement for tests to be representative of homogeneous bulk material of 6–10 cells in any direction (the homogeneous material assumption would in any case be violated for a graded structure) [20]. The variation in structure with location in the graded samples also means that the properties assessed are those of the structure, not of a bulk material.

Three uniform lattices with struts arranged in a diamond structure were made in 8 × 8 × 4 mm cuboids with unit cells of 2 mm side length where the only variable was the strut thickness, 200, 500, and 800 μm for the three lattices respectively. Three samples of a graded lattice were made with an overall size of 10 × 10 × 6 mm, also with a 2 mm unit cell size, consisting of three layers of unit cells in the *z*-direction. The strut thickness of each of these layers corresponded to the sizes of the three uniform lattices, with strut thickness increasing in each of the layers in the vertical direction. All lattices were designed using netfabb software (netfabb GmbH, Parsberg, Germany). Samples of each design were built on an EBM-S12 (Arcam AB, Mölndal, Sweden); the parameters of the fabrication process have been described in detail by Al-Bermani *et al*. [21]. In brief, structures were built from spherical particles of pre-alloyed Ti6Al4V with a diameter of 45–100 μm. The building platform was preheated to 1013 K and the lattices were built at 913 K using a speed of 200 mm/s, a beam power of 102 W, and a layer thickness of 70 μm. After building, the unmelted titanium powder was removed using a powder recycling system. The structures were cleaned in acetone for further analysis.

2.2. Structural Characterisation

In order to assess the inner structure of the lattices, samples of all types were examined using Scanning Electron Microscopy (SEM) to confirm the overall shape and surface form, and to measure the strut sizes and spacing. For a more detailed examination of the structure of the graded lattice, a micro Computed Tomography (micro-CT) scan was undertaken. An example of a graded lattice was cleaned and scanned using a Skyscan 1172 micro CT scanner (Bruker microCT, Kontich, Belgium) over an angle of 360° with one image taken every 0.7° on a camera of 2000 × 1000 pixels; the pixel size was 8.9 μm and the resolution was 25 μm. The images were taken at a voltage of 100 kV and a CuAl filter was used to improve beam quality.

2.3. Mechanical Characterisation

All samples were placed in a Hounsfield mechanical testing apparatus with, for the graded samples, the least dense layer facing upwards, and compressed at a speed of 0.25 mm/min to around 50% of the original size. The curves were corrected for the compliance of the equipment, and converted to stress-strain curves, based on the original lattice dimensions. The resulting curves were used to determine the Young's modulus (defined as $\Delta\sigma/\Delta\varepsilon$ in the first linear region of the σ-ε curve) and the 0.2% offset yield strength (defined as the stress at which the measured strain is more than 0.2% higher than that which would be expected based on linear behaviour). Statistical analysis was performed using Student's *t*-tests for the strut thickness and ANOVA and Tukey-Kramer tests for the mechanical properties.

3. Results and Discussion

3.1. Structural Characteristics

Both SEM and micro CT images confirmed that the structures had a highly regular and interconnected porosity (Figure 1, Table 1). When the designed strut size (*i.e.*, the diameter of the struts used in the input CAD model) was 800 μm there was no significant difference between the CAD model and the product, but for the smaller designed strut sizes (500 or 200 μm) those in the product were significantly higher than the CAD model ($p < 0.05$). This discrepancy occurs because when trying to build small features with sizes similar to the melted volume, the energy parameters of the beam (e.g., beam speed and beam current) become more important in determining the shape of the product than the original CAD file, and it was increasingly difficult to adjust these parameters in a way that reduced the strut size any further while retaining a good quality build (for example, absence of porosity).

Figure 1. Images of graded lattices. (**a**) Secondary electron SEM Image; (**b**) 3D reconstruction of a micro CT scan. Numbers 1–3 correspond to the smallest to the largest strut thickness respectively.

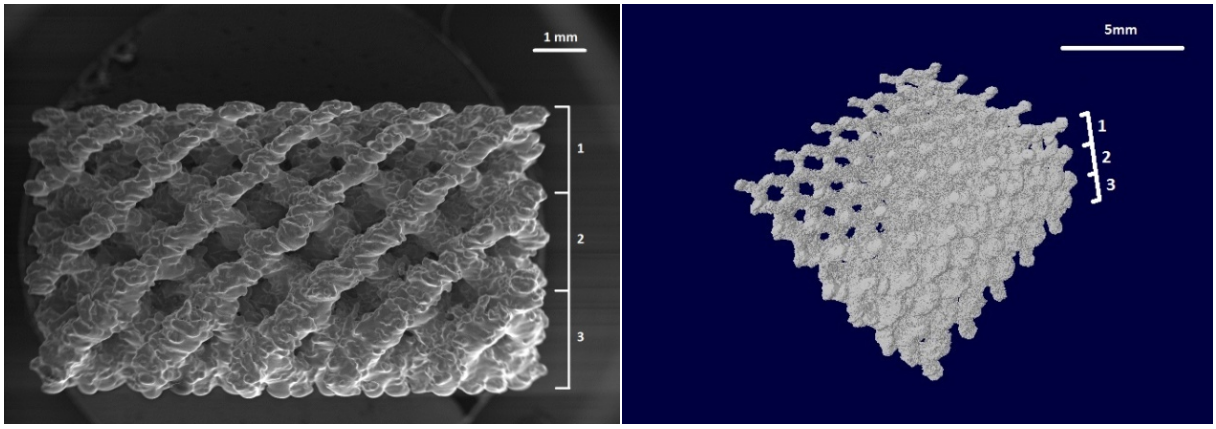

(**a**) (**b**)

Table 1. Structural and mechanical properties of all lattices (Mean ± SD).

Model strut thickness (μm)	Strut thickness (μm)	Strut spacing (μm)	Relative density (%)	Young's modulus (GPa)	Yield strength (MPa)
200	398 ± 37	827 ± 49	21 ± 0.6	1.13 ± 0.03	37 ± 1
500	600 ± 60	593 ± 57	31 ± 0.4	2.48 ± 0.40	89 ± 4
800	769 ± 42	556 ± 51	43 ± 0.1	5.38 ± 0.37	160 ± 2
Graded	-	-	33 ± 0.3	2.28 ± 0.84	46 ± 5

The average strut spacing of the three different layers is closely related to the thickness of the struts and measurements from SEM images showed a narrow distribution in all layers. These differences in strut thickness gave three different relative densities, varying from 21% at a model strut thickness of 200 μm to 43% at 800 μm.

3.2. Mechanical Behaviour

The graded and the uniform lattices were tested in uniaxial compression. The lattices behave in a highly reproducible way under compression, even after the initial failure, as shown by the example of the three traces for the repeat tests of graded lattices on the graph in Figure 2 (coloured lines). Three near-linear regions can be clearly distinguished, all followed by a point of failure and a significant, but temporary, reduction in the stress required for further compression. Visual observations during the tests confirm that the three stress maxima correspond to the collapse of individual layers in the lattice, with the layer with the thinnest struts collapsing first.

Figure 2. Stress-strain curves of three graded lattices under compressive loading. The blue, red and green lines are the curves for repeat measurements of identical graded lattice structures. The black lines indicate the predicted form of the stress strain curve calculated from the data obtained from tests on lattices of uniform structure. All curves clearly show the collapse of the individual layers and the increasing stress required to further crush the structure.

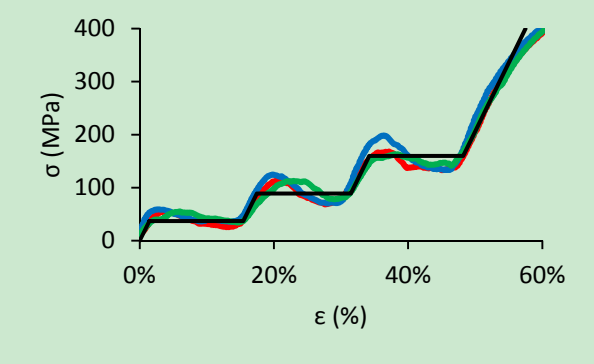

Figure 3. Comparison of the mechanical properties of the graded and uniform lattices against relative density: (**a**) Young's modulus, (**b**) yield strength. The values of the three stress peaks (corresponding to collapse of each of the layers in sequence) are shown for the graded lattice, as this shows the correlation in values with the stresses associated with the first peak in the uniform lattice structure.

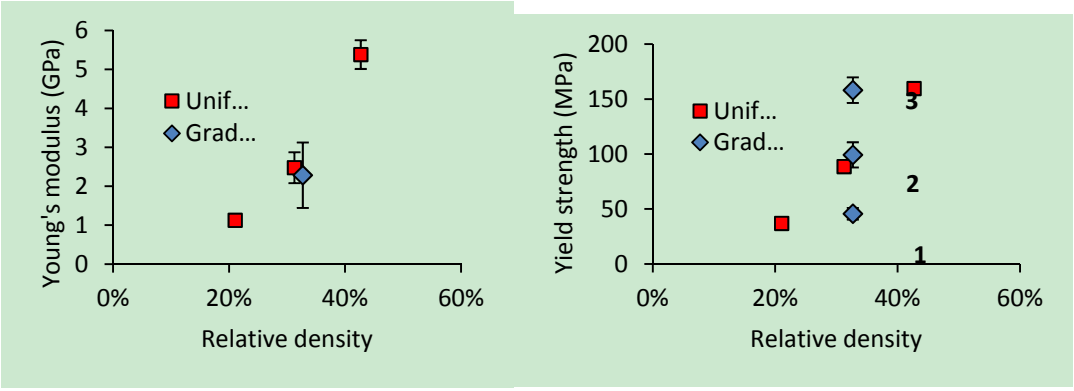

(**a**) (**b**)

As expected there is an increase in Young's modulus of the uniform lattices with increasing strut thickness (Figure 3). Statistical analysis indicated that there is a significant difference ($p < 0.05$) between all the uniform lattices and also between the graded lattice and the 800 μm uniform lattice.

The 0.2% offset yield strength was determined and was significantly higher at higher strut thickness for the uniform lattices. The yield strengths of the three layers of the graded lattice were also assessed and found to be not significantly different than the corresponding uniform lattices.

3.3. Prediction of Graded Lattice Properties

Porous metal implants have been available for over 30 years and the architecture of the porous metal is constantly changing in order to improve the stability and therefore the longevity of implants. Additive layer manufacturing techniques, such as EBM, give the designer greater control over the architecture of porous metal than ever before. In this study EBM was used to produce simple graded metal lattices in a highly reproducible manner, leading to the reproducible behaviour seen in Figure 3 to the best of our knowledge this is the first time that a structure with a porous gradient has been produced using this technique. As the mechanical behaviour of the lattices is so consistent, we can attempt to predict the behaviour of a graded lattice from the properties of its constituents using a simple procedure to estimate the location of cardinal points on the stress-strain curve.

3.3.1. Elastic Behaviour

The Young's modulus of the graded lattice can be predicted by assuming it is a simple series composite of the uniform layers of equal thickness. The prediction does not address the properties of the individual layers themselves, rather uses these experimentally-determined values as input to predict the properties of a combination of the layers together. In the iso-stress case to which this loading configuration (normal to the layers) corresponds, the rule of mixtures (slab model) may be used, leading to:

$$\frac{1}{E_{\text{Graded}}} = \frac{1}{3E_1} + \frac{1}{3E_2} + \frac{1}{3E_3} \tag{1}$$

where the subscripts 1–3 denote the different layers. Using the values that were measured for the three uniform lattices, the estimated E_{Graded} was calculated as 2.28 GPa, compared to the measured average of 2.08 GPa. Although this estimate is only representative of the initial Young's modulus (as after crushing of the first layer the remaining composite is different), we have used it for all the elastic stages due to the difficulty in estimating the modulus of the partially crushed lattice.

3.3.2. Yield and Peak Loads

The next important value is the yield strength for the initial and subsequent peaks in stress. Observations confirmed that the lattice with thinnest struts always fails first; assuming that the bonding to the neighbouring layers does not significantly affect the yield strength, we would expect that the peaks would correspond to the initial yield strengths of the uniform lattices, which were 37, 89 and 160 MPa (Table 1). The observation that there were no significant differences between the yield

strength of the uniform lattice and the corresponding layer of the graded lattice confirms this assumption.

In the graded lattice stress peaks are associated with the collapse of sequential layers. The stress would not be expected to begin to build up again until the failed layer has reached densification (when the porosity is largely removed and the metal elements are placed in direct contact). As densification is observed to occur in the uniform lattices at 43% strain, this would also be the level expected within each layer. As there are three layers, the offset between peaks should therefore be a strain of 14%. The predicted behaviour based on these points is indicated by the black line in Figure 2, and this shows very good agreement with the measured curves (at least in the details that were attempted to be predicted), indicating that this type of approach is an effective means to design a graded structure for a particular mechanical response.

3.3.3. Design of Graded Lattices

An example of where the type of design discussed here could be applied would be where a structure was required to undergo a small amount of deformation at low load, but then give a resistant structure with limited further deformation (this could, for example, be in the surgical introduction of an implant where some small amount of deformation aids conformation to the existing tissue, or for a protective application where deformation under small loads would protect against low energy impacts; in either case a rapid development of full properties would be required). In this situation a lattice could be constructed of a small number of layers of low density, combined with a larger number of layers where the density resulted in suitable properties. These results pertain to quasi-static conditions. If loading was to occur dynamically, such as under impact, then it may be that the first layer of cells would undergo deformation initially, even if this was not the lowest strength layer, as other layers would be supported by their inertia. In such circumstances there may be freedom to extend these design principles to produce lattices where the stress required for failure of further layers does not always increase, although in such a situation it is likely that the properties determined from tests on uniform lattices under representative conditions would be required.

4. Conclusions

EBM can be used to produce lattices with graded porosity. Mechanical properties of the different layers are reproducible (maximum standard deviation from tests on three samples of 16% for Young's modulus and 4% for yield strength) and it is possible to obtain a good estimate of the behaviour of a regular lattice graded across a series of layers when tested along the direction of grading by combining the properties of uniform lattices of the same design in series. Such a procedure could be very useful in designing lattice response tuned to specific mechanical requirements, such as for orthopaedic implants.

Acknowledgments

The authors would like to acknowledge Fatos Derguti and Lampros Kourtis of the Mercury Centre for their help in the fabrication process, Leslie Coulton of the Mellanby Centre for his help with the CT

analysis, and Orthopaedic Research UK (ORUK) for funding for this project. The views expressed here do not necessarily represent those of ORUK.

Author Contributions

WvG as the primary author of the paper, and performed most of the experimental work and data analysis reported. EHN fabricated the lattices using EBM. GCR and RG supervised the work and discussed the results and analysis with the other authors.

Conflicts of Interest

The authors declare no conflict of interest.

References

1. Ashby, M.F.; Evans, A.G.; Fleck, N.A.; Gibson, L.J.; Hutchinson, J.W.; Wadley, H.N.G. *Metal Foams: A Design Guide*; Butterworth-Heinemann: Boston, MA, USA, 2000.
2. Banhart, J. Manufacture, Characterisation and Application of Cellular Metals and Metal Foams. *Prog. Mat. Sci*. **2001**, *46*, 599–632.
3. Goodall, R.; Mortensen, A. Porous Metals. In *Physical Metallurgy*, 5th ed.; Laughlin, D., Hono, K., Eds.; Elsevier: Amsterdam, The Netherlands, 2014; In press.
4. Gibson, L.J.; Ashby, M.F. *Cellular Solids*, 2nd ed.; Cambridge University Press: Cambridge, UK, 1997.
5. Despois, J.-F.; Mueller, R.; Mortensen, A. Uniaxial Deformation of Microcellular Metals. *Acta Mater.* **2006**, *54*, 4129–4142.
6. Goodall, R.; Despois, J.-F.; Marmottant, A.; Salvo, L.; Mortensen, A. The Effect of Preform Processing on Replicated Aluminium Foam Structure and Mechanical Properties. *Scripta Mater.* **2006**, *54*, 2069–2073.
7. Wadley, H.N.G. Multifunctional Periodic Cellular Materials. *Phil. Trans. R. Soc. A* **2006**, *364*, 31–68.
8. Abdulla, T.; Yerokhin, A.; Goodall, R. Effect of Plasma Electrolytic Oxidation Coating on the Specific Strength of Open-cell Aluminium Foams. *Mater. Des.* **2011**, *32*, 3742–3749.
9. Abdulla, T.; Yerokhin, A.; Goodall, R. Enhancement in specific strength of open cell aluminium foams through plasma electrolytic oxidation treatment. *Scripta Mater.* **2014**, *75*, 38–41.
10. Heinl, P.; Rottmair, A.; Körner, C.; Singer, R.F. Cellular Titanium by Selective Electron Beam Melting. *Adv. Eng. Mater.* **2007**, *9*, 360–364.
11. Murr, L.E.; Amato, K.N.; Li, S.J.; Tian, Y.X.; Cheng, X.Y.; Gaytan, S.M.; Martinez, E.; Shindo, P.W.; Medina, F.; Wicker, R.B. Microstructure and mechanical properties of open-cellular biomaterials prototypes for total knee replacement implants fabricated by electron beam melting. *J. Mech. Behav. Biomed. Mater.* **2011**, *4*, 1396–1411.
12. Heinl, P.; Muller, L.; Korner, C.; Singer, R.F.; Muller, F.A. Cellular Ti–6Al–4V structures with interconnected macro porosity for bone implants fabricated by selective electron beam melting. *Acta Biomater.* **2008**, *4*, 1536–1544.

13. Ponader, S.; Vairaktaris, E.; Heinl, P.; Wilmowsky, C.V.; Rottmair, A.; Körner, C.; Singer, R.F.; Holst, S.; Schlegel, K.A.; Neukam, F.W.; *et al*. Effects of topographical surface modifications of electron beam melted Ti-6Al-4V titanium on human fetal osteoblasts. *J. Biomed. Mater. Res. A* **2008**, *84*, 1111–1119.
14. Ponader, S.; Wilmowsky, C.V.; Widenmayer, M.; Lutz, R.; Heinl, P.; Körner, C.; Singer, R.F.; Nkenke, E.; Neukam, F.W.; Schlegel, K.A. *In vivo* performance of selective electron beam-melted Ti-6Al-4V structures. *J. Biomed. Mater. Res. A* **2009**, *92*, 56–62.
15. Biemond, J.E.; Hannink, G.; Jurrius, A.M.G.; Verdonschot, N.; Buma, P. *In Vivo* Assessment of Bone Ingrowth Potential of Three-Dimensional E-Beam Produced Implant Surfaces and the Effect of Additional Treatment by Acid Etching and Hydroxyapatite. *Coat. J. Biomater. Appl.* **2012**, *26*, 861–875.
16. Brothers, A.H.; Dunand, D.C. Density-Graded Cellular Aluminium. *Adv. Eng. Mater.* **2006**, *8*, 805–809.
17. Brothers, A.H.; Dunand, D.C. Mechanical Properties of a Density-Graded Replicated Aluminium Foam. *Mat. Sci. Eng. A* **2008**, *489*, 439–443.
18. Zaragoza, G.; Goodall, R. Metal Foams with Graded Pore Size for Heat Transfer Applications. *Adv. Eng. Mater.* **2013**, *15*, 123–128.
19. Karageorgiou, V.; Kaplan, D. Porosity of 3D Biomaterial Scaffolds and Osteogenesis. *Biomaterials* **2005**, *26*, 5474–5491.
20. Andrews, E.W.; Gioux, G.; Onck, P.; Gibson, L.J. Size Effects in Ductile Cellular Solids. Part II: Experimental Results. *Int. J. Mech. Sci.* **2001**, *43*, 701–713.
21. Al-Bermani, S.S.; Blackmore, M.L.; Zhang, W.; Todd, I. The origin of microstructural diversity, texture and mechanical properties in electron beam melted Ti-6Al-4V. *Met. Mater. Trans. A* **2010**, *41*, 3422–3434.

© 2014 by the authors; licensee MDPI, Basel, Switzerland. This article is an open access article distributed under the terms and conditions of the Creative Commons Attribution license (http://creativecommons.org/licenses/by/3.0/).